

Growth- and substrate-dependent transcription of formate dehydrogenase and hydrogenase coding genes in *Syntrophobacter fumaroxidans* and *Methanospirillum hungatei*

Petra Worm, Alfons J. M. Stams, Xu Cheng and Caroline M. Plugge

Correspondence
Caroline M. Plugge
caroline.plugge@wur.nl

Laboratory of Microbiology, Wageningen University, Dreijenplein 10, 6703 HB Wageningen, The Netherlands

Transcription of genes coding for formate dehydrogenases (*fdh* genes) and hydrogenases (*hyd* genes) in *Syntrophobacter fumaroxidans* and *Methanospirillum hungatei* was studied following growth under different conditions. Under all conditions tested, all *fdh* and *hyd* genes were transcribed. However, transcription levels of the individual genes varied depending on the substrate and growth conditions. Our results strongly suggest that in syntrophically grown *S. fumaroxidans* cells, the [FeFe]-hydrogenase (encoded by Sfum_844-46), FDH1 (Sfum_2703-06) and Hox (Sfum_2713-16) may confurcate electrons from NADH and ferredoxin to protons and carbon dioxide to produce hydrogen and formate, respectively. Based on bioinformatic analysis, a membrane-integrated energy-converting [NiFe]-hydrogenase (Mhun_1741-46) of *M. hungatei* might be involved in the energy-dependent reduction of CO₂ to formylmethanofuran. The best candidates for F₄₂₀-dependent N⁵,N¹⁰-methyl-H₄ MPT and N⁵,N¹⁰-methylene-H₄MPT reduction are the cytoplasmic [NiFe]-hydrogenase and FDH1. 16S rRNA ratios indicate that in one of the triplicate co-cultures of *S. fumaroxidans* and *M. hungatei*, less energy was available for *S. fumaroxidans*. This led to enhanced transcription of genes coding for the Rnf-complex (Sfum_2694-99) and of several *fdh* and *hyd* genes. The Rnf-complex probably reoxidized NADH with ferredoxin reduction, followed by ferredoxin oxidation by the induced formate dehydrogenases and hydrogenases.

Received 21 July 2010
Revised 23 September 2010
Accepted 24 September 2010

INTRODUCTION

In anaerobic environments, degradation of complex organic matter to carbon dioxide and methane is performed by a consortium of micro-organisms that each have a specific metabolic function (McInerney *et al.*, 2008; Schink & Stams, 2006). Important metabolic intermediates are organic acids such as propionate and butyrate. Their degradation depends on syntrophy between bacteria and methanogenic archaea. Even under optimal growth conditions, available free energy is low and has to be shared by all partners in the consortia (Schink & Stams, 2006).

Syntrophobacter fumaroxidans is a deltaproteobacterium that degrades propionate in syntrophic association with the hydrogen- and formate-using *Methanospirillum hungatei* or *Methanobacterium formicicum* (Harmsen *et al.*, 1998). Cultivation and biochemical experiments indicate that both hydrogen and formate transfer are important

interspecies electron transfer mechanisms (de Bok *et al.*, 2002a, b; Dong & Stams, 1995). Propionate degradation in the absence of an external electron acceptor requires low hydrogen and formate concentrations (1 Pa and 10 µM) to gain energy for growth (Schink & Stams, 2006). *M. hungatei* and *M. formicicum* are able to maintain such low concentrations. Although syntrophic partners regulate their metabolism to grow together, there are conflicting needs.

S. fumaroxidans metabolizes propionate via the methylmalonyl-CoA pathway (Plugge *et al.*, 1993). Electrons are generated in three steps: (i) succinate to fumarate, (ii) malate to oxaloacetate, and (iii) pyruvate to acetyl-CoA plus CO₂. These electrons convert together with protons or protons plus CO₂ to H₂ and formate, respectively. Subsequently hydrogen and formate are transferred to and further metabolized by the methanogenic partner. In pure culture, the bacterium is able to use fumarate and sulfate as electron acceptors (Harmsen *et al.*, 1998). *S. fumaroxidans* can also grow with hydrogen and fumarate, formate and fumarate, and even by fumarate fermentation (Harmsen *et al.*, 1998). The exact mechanism

Abbreviations: CoMf/CoMh, *S. fumaroxidans* grown in co-culture with *M. hungatei* JF-1/*M. formicicum* JF-1; C_t, cycle threshold.

Three supplementary figures are available with the online version of this paper.

of NADH oxidation and terminal reduction of protons and/or CO₂ in *S. fumaroxidans* remains unclear. Recent analysis of the genome of *S. fumaroxidans* suggests that novel energy-transforming reactions are involved in syntrophic propionate degradation (Müller *et al.*, 2010) (Table 1). To drive the endergonic oxidation of succinate, involvement of a periplasmic formate dehydrogenase (FDH2) and hydrogenase (Hyn), cytochrome *b*:quinone oxidoreductases and a menaquinone loop was proposed. Furthermore, Schut & Adams (2009) proposed that a bifurcating [FeFe]-hydrogenase (FeHyd) in *S. fumaroxidans* might simultaneously use electrons from NADH and reduced ferredoxin in a 1:2 ratio to produce hydrogen analogously to *Thermotoga maritima*. A similar function was proposed for formate dehydrogenase-1 (FDH1) and a [NiFe]-hydrogenase (Hox) (Müller *et al.*, 2010). It was also hypothesized that an Rnf-complex is used to reoxidize NADH by ferredoxin reduction with the use of a proton motive force (Müller *et al.*, 2010). In addition, the genome of *S. fumaroxidans* contains genes that could code for a cytoplasmic [NiFe]-hydrogenase (Frh), two cytoplasmic [NiFeSe]-hydrogenases (Hdr and Fnr), a [NiFe]-hydrogenase maturation protein (NiFeHydMat), and two cytoplasmic formate dehydrogenases (FDH3 and -4). Furthermore, a gene cluster with similarity to those coding for cytoplasmic-oriented membrane proteins to interconvert hydrogen plus CO₂ and formate, referred to as a formate hydrogen lyase complex, is present. These genes show similarity with those coding for a formate dehydrogenase (FHL-F), a hydrogenase (FHL-H) and several iron-sulfur cluster binding proteins (Müller *et al.*, 2010). Unlike the FHL of *Escherichia coli* (Bagramyan & Trchounian, 2003), genes coding for membrane-integrated subunits were lacking in the FHL coding gene cluster of *S. fumaroxidans*.

M. hungatei uses the hydrogen and formate generated by *S. fumaroxidans* to form methane, and electrons are required in four reduction steps: the conversion of carbon dioxide to formylmethanofuran, N⁵,N¹⁰-methyl-H₄MPT to N⁵,N¹⁰-methylene-H₄MPT, N⁵,N¹⁰-methylene-H₄MPT to N⁵-methyl-H₄MPT and methyl coenzyme-M to methane and coenzyme-M (Schwörer & Thauer, 1991). In *M. hungatei*, hydrogenases and formate dehydrogenases oxidize hydrogen and formate to supply electrons for the reduction reactions. Although the genome sequence of *M. hungatei* is available, the gene analysis of its formate dehydrogenase and hydrogenase coding genes (*fdh* and *hyd* genes, respectively) has not been described. The genome of *M. formicicum* has not been sequenced yet.

Here, we studied the novel energy-transforming reactions involved in syntrophic propionate degradation that were recently hypothesized (Müller *et al.*, 2010; Sieber *et al.*, 2010). To survey the molecular basis of syntrophic interactions, transcription of the genes involved was studied in detail (*fdh* and *hyd* genes, *NiFeHydMat*, *rnfC*, *fhl-F* and *fhl-H*) in *S. fumaroxidans* grown with different substrates, in both pure cultures and co-cultures with *M. hungatei* or *M. formicicum*. To further study the regulation of the

syntrophic interaction between *S. fumaroxidans* and *M. hungatei*, *fdh* and *hyd* genes of *M. hungatei* were analysed by using bioinformatics and the transcription of these genes in cells grown in pure and co-culture was analysed.

METHODS

Micro-organisms and growth conditions. *S. fumaroxidans* MPOB (DSM 10017), the methanogenic archaea *M. hungatei* JF-1 (DSM 864) and *M. formicicum* JF-1 (DSM 1535) were used in this study. *S. fumaroxidans* was grown in either pure culture or co-culture with one of the methanogenic archaea (CoMh, with *M. hungatei* JF-1; CoMf, with *M. formicicum* JF-1). All cultures were grown at 37 °C in anaerobic liquid medium as described previously (Stams *et al.*, 1993). Micro-organisms were cultured in 120 ml or 1 l flasks with 50 or 500 ml medium, respectively, and a headspace of 1.7 atm N₂/CO₂ or H₂/CO₂ (80:20, v/v). *S. fumaroxidans* and *M. hungatei* cells were grown under different conditions in triplicate (Table 2). Growth was followed by measuring OD₆₆₀ and/or methane formation. Cells were harvested in the exponential phase.

RNA extraction and reverse transcription. *fdh* and *hyd* genes in the genome of *M. hungatei* were analysed by using the same bioinformatic tools as described previously for *S. fumaroxidans* (Müller *et al.*, 2010). Twin-arginine translocation (Tat) motifs in the N-termini were identified by using PRED-SIGNAL (Bagos *et al.*, 2009) to predict the cell localization of proteins in *M. hungatei* cells. Cultures were harvested by centrifugation at 3800 g at 4 °C for 20 min. Cell pellets were resuspended in RNA stabilization solution RNeasy (Ambion), incubated at 4 °C overnight and stored at -20 °C. Stored cells were centrifuged at 3800 g at 4 °C for 10 min and the resulting cell pellet was resuspended in 125 µl RNase-free water and 375 µl TRIzol Reagent (Invitrogen), transferred to a tube containing 0.1 mm silica beads and homogenized at 4.5 m s⁻¹ for 30 s in a FastPrep-24 (MP Biomedicals). Tubes were incubated at 20 °C for 5 min and 0.1 ml chloroform was added followed by 15 s manual shaking. After incubation at 20 °C for 5 min, the suspension was centrifuged at 9500 g at 4 °C for 15 min. The aqueous phase with an equal amount of 70 % ethanol was transferred to an RNeasy mini spin column (Qiagen) and on-column DNase digestion with RNase-free DNase I (Qiagen) was performed according to the manufacturer's instructions. RNA was ultimately eluted in 60 µl RNase-free water and RNA integrity was confirmed by an Experion RNA StdSens Chip (Bio-Rad) using the Bio-Rad Experion system. Copy DNA was synthesized by SuperScript III reverse transcriptase (Invitrogen) according to the manufacturer's instructions with random decamers (Ambion). To distinguish genomic DNA from cDNA in qPCR, RT-minus controls were prepared in a similar reaction mixture in which SuperScript III was replaced with water.

Primer design and qPCR. Primers were designed with Primer Premier 5 software and synthesized by BioLegio or Eurogentec (Table 1). The optimal melting temperature (58 °C) of each primer set was experimentally verified with genomic DNA from *S. fumaroxidans*, *M. hungatei* or *M. formicicum* as template. Genomic DNA was isolated with the bead-beat and phenol/chloroform-based DNA extraction method (van Doesburg *et al.*, 2005). qPCR was performed with the MyiQ single colour real-time PCR detection system (Bio-Rad). Each 25 µl reaction mixture contained 5 µl 20 × diluted cDNA, 12.5 µl 2 × QuantiTect SYBR Green PCR mix (Qiagen) and 0.3 µM each primer. Thermocycling conditions were as follows: 95 °C for 10 min, 40 cycles of 95 °C for 15 s, 58 °C for 30 s and 72 °C for 30 s, with fluorescence detection at the end of each extension step. Amplification was immediately followed by a melting programme consisting of 95 °C for 1 min, 55 °C for 1 min and a step-wise temperature increase of 0.5 °C per 10 s with fluorescence detection at each temperature transition. Melting curve peaks for each primer pair indicated that

Table 1. RT qPCR primers designed to amplify cDNA of target gene transcripts in *S. fumaroxidans* and *M. hungatei*

Specific genes are listed with the corresponding locus tag (<http://img.jgi.doe.gov>, version 2.9) and the predicted metal content and cell localization of the formate dehydrogenase and hydrogenases. Primers targeting cDNA of 16S rRNA from *M. formicicum* used for calculations of the ratio of 16S rRNA from *M. formicicum* and *S. fumaroxidans* are also included. –, Localization unknown or no metal content.

Gene	Locus tag (IMG)	Localization	Metal content	Primer name	Primer sequence (5'–3')
<i>fdh-1</i>	Sfum_2706, Sfum_2705*	Cytoplasm	W and Se†	SF_fdh1-fw SF_fdh1-rv	CGG CGT CCC GTG AGT T GGC AGG GTG CTC TAC CAG TAT
<i>fdh-2</i>	Sfum_1274, Sfum_1273*	Periplasm	W and Se†	SF_fdh2-fw SF_fdh2-rv	TGG TGC CAG CAT TCG GTG ATG TTC CCC AGG AGC AGC
<i>fdh-3</i>	Sfum_3509	Periplasm	W or Mo	SF_fdh3-fw SF_fdh3-rv	GGA CAT CTC GCG TTT GGA C CTC GCC TTG ACT TTC ACC TCT
<i>fdh-4</i>	Sfum_0031, Sfum_0030*	Periplasm	W or Mo and Se	SF_fdh4-fw SF_fdh4-rv	CTA CCA TAC GCG GAC CCA G CGA TTT CAC CCG GAC TTT G
<i>fehyd-1</i>	Sfum_0844	Periplasm	Fe	SF_fehyd-fw SF_fehyd-rv	CCC GAG GAA TAC GAC GCT TCA CGC CGC CAG AAG C
<i>hyn</i>	Sfum_2952	Cytoplasm	Ni and Fe	SF_hyn-fw SF_hyn-rv	ACG TCG GCA AAG GCA ATA C GTC GTT CAG ACC CGC TCC
<i>frh</i>	Sfum_2221	Cytoplasm	Ni and Fe	SF_frh-fw SF_frh-rv	GTT CGC GGT TGA CTT TGC CCT CAG CCT GCC ATC GTA GA
<i>hox</i>	Sfum_2716	Cytoplasm	Ni and Fe	SF_hox-fw SF_hox-rv	GGT CTG CTG AGG GTG ATG G GGC GTC CGT GCC GTA T
<i>hdr</i>	Sfum_3537*	Cytoplasm	Ni, Fe and Se	SF_hdr-fw SF_hdr-rv	GGC ACC ACC CAC AAC CTC CGC ACG GCC ATC TCC A
<i>fnr</i>	Sfum_3954*	Cytoplasm	Ni, Fe and Se	SF_fnr-fw SF_fnr-rv	GCC CGT GGC AGC ATC A GCA GAA TCT TGT CTT CGG AGT G
<i>rnfC</i>	Sfum_2699	Cytoplasm	–	SF_rnfc-fw SF_rnfc-rv	ACC GAG CAT CTG CCC ATA G GAA CCG AAG TGT TGA AGA AGG A
<i>fhl-f</i>	Sfum_1795, Sfum_1796	Cytoplasm	Mo or W and Se	SF_fhlf-fw SF_fhlf-rv	GCG GGT GCG GGT TCT A CGG TTG AGT CAG ACG ATT GG
<i>fhl-h</i>	Sfum_1791	Cytoplasm	Ni, Fe	SF_fhlh-fw SF_fhlh-rv	AAG GTG GAG CCC AAA GCA CGG TCC CAG GTT GTG AGT G
<i>NiFe-hyd-mat</i>	Sfum_4014	Cytoplasm	–	SF_mat-fw SF_mat-rv	CGG TCT TTT CGG CTC ACA CGA TAG TTG TCC ACC ACT TCC T
16S rRNA	Sfum_R0013, Sfum_R0015	–	–	SF_16S-fw SF_16S-rv	ACG CTG TAA ACG ATG AGC ACT A GAT GTC AAG CCC AGG TAA GGT
<i>fdh-1</i>	Mhun_1813	Cytoplasm	W or Mo	MHfdh1-fw MHfdh1-rv	CGC AGC AGC AAT GGG ATA CGT AGG ACG GGG TGA GTG A
<i>fdh-2</i>	Mhun_1833	Cytoplasm	W or Mo	MHfdh2-fw MHfdh2-rv	CGG TGA ATG AAG GAA AAC TCT G CGG GCT GTG GAT AAA CTG G
<i>fdh-3</i>	Mhun_2021	Cytoplasm	W or Mo	MHfdh3-fw MHfdh3-rv	AAG AAG ACG GTT GAG AAC TAC G GTT TCC AGT CAG AAG AGC AAG A
<i>fdh-4</i>	Mhun_2023	Cytoplasm	W or Mo	MHfdh4-fw MHfdh4-rv	GTC ACC GAA CTG ACC ACC G GCA CCC ATA TCA CAA GCA CC
<i>fdh-5</i>	Mhun_3238	Cytoplasm	W or Mo	MHfdh5-fw MHfdh5-rv	ACC CTA TCA GCG TTC TCC G AAA CTC GTG AGC ATA AGT CCC T
<i>ech</i>	Mhun_1745	Periplasm	Ni and Fe	MHech-fw MHech-rv	CTT CCT GAG CCC ATT CAT CTT ATA GTC CTT GTA ATC ACG CTT TTC
<i>frc</i>	Mhun_2332	Cytoplasm	Ni and Fe	MHfrc-fw MHfrc-rv	ATG CGG GAA TAA TTG AGC G ATA CCA CAA ACA CGG GAT GAG
<i>mbh</i>	Mhun_2590	Periplasm	Ni and Fe	MHmbh-fw MHmbh-rv	GCA TCC ACC TAC TCA AAC CAG TGC CCG ACA ACA GCC AC
<i>M. hungatei</i> 16S rRNA	Mhun_R0001, Mhun_R0072, Mhun_R0068, Mhun_R0027	–	–	MH16S-fw MH16S-rv	TCG TGC TGA CTG GAA TGT TAT CAG ACT CAT CCT GAA GCG AC
<i>M. formicicum</i> 16S rRNA	NR_025028‡	–	–	MF16S-fw MF16S-rv	CTT CGG GGT CGT GGC GTA C CAG ATT ACT GGC TTG GTG GG

*Selenocysteine residues predicted (Müller *et al.*, 2010).

†Metal content of the purified formate dehydrogenases as determined by de Bok *et al.* (2003).

‡GenBank accession no. of the 16S rRNA gene from *M. formicicum*.

single amplicon sizes were generated. The optimal baseline was calculated by using the Bio-Rad MyiQ system software version 1.0 and generated threshold cycle (C_t) values. A second arbitrary baseline was manually defined and the amplification efficiency for each individual reaction was calculated from the kinetic curve (Liu & Saint, 2002). Gene transcription values were normalized to 16S rRNA levels of the corresponding organism. At least three technical replicates were performed for each biological replicate (with the exception of in *M. hungatei* cells grown on formate in which transcription levels of *fdh-3* and *ech* were below the detection limit). Relative transcription levels were calculated from C_t values that were above the detection limit of 35 cycles. Template-minus controls performed for each primer and RT-minus controls performed for each sample were below this detection limit. Outliers in technical replicates were determined with a Grubbs' test (Burns *et al.*, 2005). Q-Q plots with \log_{10} of relative transcription levels showed a normal distribution. The mean \pm SD of technical replicates of three biological replicates were calculated. Pair-wise *t*-tests were performed to find the least significant difference between any of the means at $P < 0.05$ or $P < 0.01$. To examine the influence of the growth phase on the gene transcription profiles, *S. fumaroxidans* was grown on fumarate plus formate and on fumarate plus hydrogen, and harvested in the lag, exponential and stationary phases of growth. To compare gene transcription profiles between growth phases, the levels for exponential and stationary phase were normalized by multiplying by a factor that was calculated by taking the difference in the mean of all genes in that condition. Differences in 16S rRNA levels in the exponential and stationary phase were on average 285- and 303-fold lower than in the lag phase in the case of cells grown on hydrogen and fumarate, and 55- and 50-fold lower in the case of cells grown on formate and fumarate. Pair-wise *t*-tests revealed that no significant differences ($P < 0.01$) in transcription profiles between cells grown in the lag, exponential and stationary phase were found (Supplementary Fig. S1, available with the online version of this paper). Therefore, all other measurements were done with cells in the exponential growth phase.

RESULTS

Growth of *S. fumaroxidans* and *M. hungatei* on different substrates

All *S. fumaroxidans* cultures grew well and yielded sufficient RNA (0.18–18 μ g) to determine transcription

levels of genes of interest, as did *M. hungatei* grown on H_2/CO_2 . *M. hungatei* grown on formate yielded enough RNA (2–4 μ g) to determine most of the gene transcription levels (Fig. 1). The ratio of *M. hungatei* 16S rRNA: *S. fumaroxidans* 16S rRNA in CoMh1 was 10 times higher than in CoMh2 and -3, whereas the generation times of the three co-cultures were comparable (Table 2).

Transcription of *fdh* and *hyd* genes in *S. fumaroxidans*

Under all conditions tested, all *fdh* and *hyd* genes were transcribed in *S. fumaroxidans*. However, transcription levels of the individual *fdh* and *hyd* genes varied depending on the substrate and growth conditions. Transcription levels of *fdh-1* and -2 (encoding FDH1 and -2, respectively) were 3.0–1700 times higher ($P < 0.01$) in all conditions (Fig. 2b–d) than *fdh-3* and -4 (encoding FDH3 and -4, respectively) with the exception of cells grown in co-culture with *M. hungatei*. Transcription levels of *fdh-1* were 11–39 times ($P < 0.01$) higher in cells grown in co-culture with *M. formicicum* and 2.3–8.3 times ($P < 0.05$) higher in co-culture with *M. hungatei* than in cells grown in pure culture (Fig. 2a). *fdh-2* (encoding FDH2) was transcribed at 2.7–21 times ($P < 0.01$) higher levels in *S. fumaroxidans* cells grown with fumarate fermentation, on propionate plus sulfate or on propionate in co-cultures with *M. hungatei* or *M. formicicum* than in cells grown with fumarate as electron acceptor and hydrogen, formate or propionate as electron donor (Fig. 2b). *feh* (encoding FeHyd) was transcribed at 2.0–28 times ($P < 0.01$) higher levels in cells grown with propionate as the substrate in pure cultures with fumarate or sulfate as electron donor or in co-cultures with a methanogenic partner than in cells grown with fumarate fermentation, hydrogen plus fumarate or formate plus fumarate (Fig. 2h). Transcription levels of *fhl-f* (encoding FHL-F) were 4.1–44 times ($P < 0.01$)

Table 2. Growth conditions and generation times of *S. fumaroxidans* and *M. hungatei* from triplicate cultures used in this study

Code	Organism or co-culture	Substrate	Generation time (days)*		
			Replicate 1	Replicate 2	Replicate 3
PF	<i>S. fumaroxidans</i> †	20 mM propionate + 60 mM fumarate	1.4	1.3	1.4
F	<i>S. fumaroxidans</i> †	30 mM fumarate	3.7	2.9	2.6
HF	<i>S. fumaroxidans</i> †	30 mM fumarate + H_2/CO_2 (80:20, v/v)	2.1	2.2	2.2
FF	<i>S. fumaroxidans</i> †	30 mM fumarate + 30 mM formate	2.7	1.4	1.4
PS	<i>S. fumaroxidans</i> ‡	30 mM propionate + 30 mM sulfate	9.3	5.9	7.0
CoMh	<i>S. fumaroxidans</i> + <i>M. hungatei</i> ‡	30 mM propionate	5.8 (45)	4.1 (4.7)	3.8 (6.9)
CoMf	<i>S. fumaroxidans</i> + <i>M. formicicum</i> ‡	30 mM propionate	8.2 (7.3)	6.8 (2.9)	8.4 (1.6)
For	<i>M. hungatei</i> ‡	30 mM formate + 1 mM acetate	0.6	0.5	0.4
H_2	<i>M. hungatei</i> ‡	H_2/CO_2 (80:20, v/v) + 1 mM acetate	1.8	2.2	1.7

*The ratio of 16S rRNA from *M. hungatei* or *M. formicicum*: 16S rRNA from *S. fumaroxidans* is shown in parentheses.

†Culture volume, 50 ml.

‡Culture volume, 500 ml.

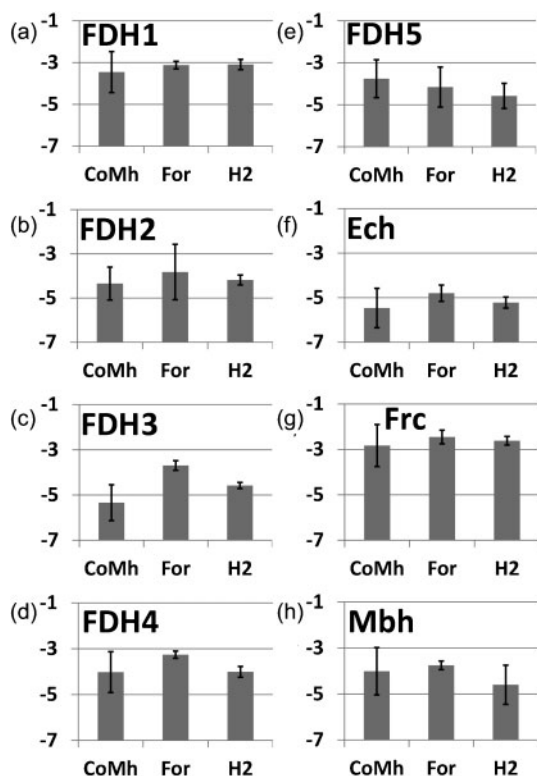


Fig. 1. Transcription of *M. hungatei* genes coding for formate dehydrogenases (a–e) and hydrogenases (f–h). Culture conditions were *S. fumaroxidans* grown in co-culture with *M. hungatei* (CoMh), with formate (For) and with hydrogen (H2). Each column shows the mean \pm SD of three replicate cultures for each growth condition; the \log_{10} relative transcription levels are shown on the y-axis.

higher in cells grown in co-culture with a methanogen than in cells grown in pure culture (Fig. 2f). *fhl-h* (encoding FHL-H) transcription levels were also higher in co-cultures than in cells grown in pure culture (3.2–12 times, $P < 0.01$) with the exception of those grown on propionate plus sulfate (Fig. 2g). The transcription level of the gene coding for Hyn was 3.2–9.7 times ($P < 0.01$) lower in co-cultures with *M. formicicum* than in pure cultures (Fig. 2i). Transcription of *hox* (encoding Hox) was 3.3–9.1 times ($P < 0.01$) higher in cells grown on propionate in pure culture with sulfate reduction or in co-culture with methanogens than in cultures grown with fumarate as an electron acceptor (Fig. 2k). Transcription of the gene coding for the [NiFe]-hydrogenase maturation protein (NiFeHydMat) was not significantly different ($P \geq 0.01$) between all growth conditions tested (Fig. 2n). Genes coding for the Rnf-complex, the periplasmic Hyn, the cytoplasmic Hox, FDH3 and FDH4 were transcribed at levels that were 13–1700 times ($P < 0.01$) higher in CoMh1 than in CoMh2 and -3, with the exception that the *fdh-4* transcription level was also high in CoMh2 (Fig. 3).

Gene analysis of *fdh* and *hyd* genes in *M. hungatei*

Analysis of the genome sequence of *M. hungatei* (<http://img.jgi.doe.gov>, version 2.9) indicated the presence of five F_{420} -reducing formate dehydrogenases (FDH1–5) and three hydrogenases. The three hydrogenases include a membrane-integrated ion-translocating energy-converting [NiFe]-hydrogenase (Ech), a cytoplasmic F_{420} -reducing hydrogenase (Frc), and an ion-translocating membrane-bound [NiFe]-hydrogenase (Mbh) (Hendrickson & Leigh, 2008; Thauer *et al.*, 2008).

Transcription of *fdh* and *hyd* genes in *M. hungatei*

Under all conditions tested, all *fdh* and *hyd* genes were transcribed in *M. hungatei* and no differences ($P < 0.01$) in transcription levels were observed between *M. hungatei* cells grown with hydrogen and cells grown with formate (Fig. 1). In all conditions, *frc* (encoding Frc) transcription levels were 3.0–430 times ($P < 0.05$) higher than other *fdh* and *hyd* genes (Fig. 1g). In all tested conditions, transcription levels of *mbh* (encoding Mbh) were 4.2–29 times ($P < 0.01$) higher than transcription levels of the gene coding for the other putative ion-translocating hydrogenase Ech (Fig. 1f, h). Transcription levels of all *M. hungatei* genes in CoMh1 were 5.0–130 times ($P < 0.05$) higher than of those in CoMh2 and -3, with the exception of *ech* and *mbh*.

DISCUSSION

Transcription of genes involved in electron-generating steps of the methyl-malonyl-CoA pathway

The energetically most difficult step in the methyl-malonyl-CoA pathway is the oxidation of succinate to fumarate (Stams & Plugge, 2009). Recently, Müller *et al.* (2010) proposed that a periplasmic formate dehydrogenase (FDH2), a hydrogenase (Hyn), cytochrome *b*:quinone oxidoreductases and a menaquinone loop drive the endergonic oxidation of succinate. During propionate degradation in co-culture with methanogens or in pure culture with sulfate as the electron acceptor, the endergonic succinate oxidation step is performed. With fumarate as an electron acceptor (hydrogen plus fumarate, formate plus fumarate, propionate plus fumarate and fumarate only), a reversed mechanism is needed. Our results indicate that both Hyn and FDH2 play a role in fumarate reduction and in succinate oxidation and that FDH2 might play a more important role during endergonic succinate oxidation. This would mean that in co-cultures, both formate and hydrogen are used for interspecies electron transfer, but that from the succinate oxidation step, more formate is generated than hydrogen.

When *S. fumaroxidans* degrades propionate, NADH and reduced ferredoxin are generated during malate and

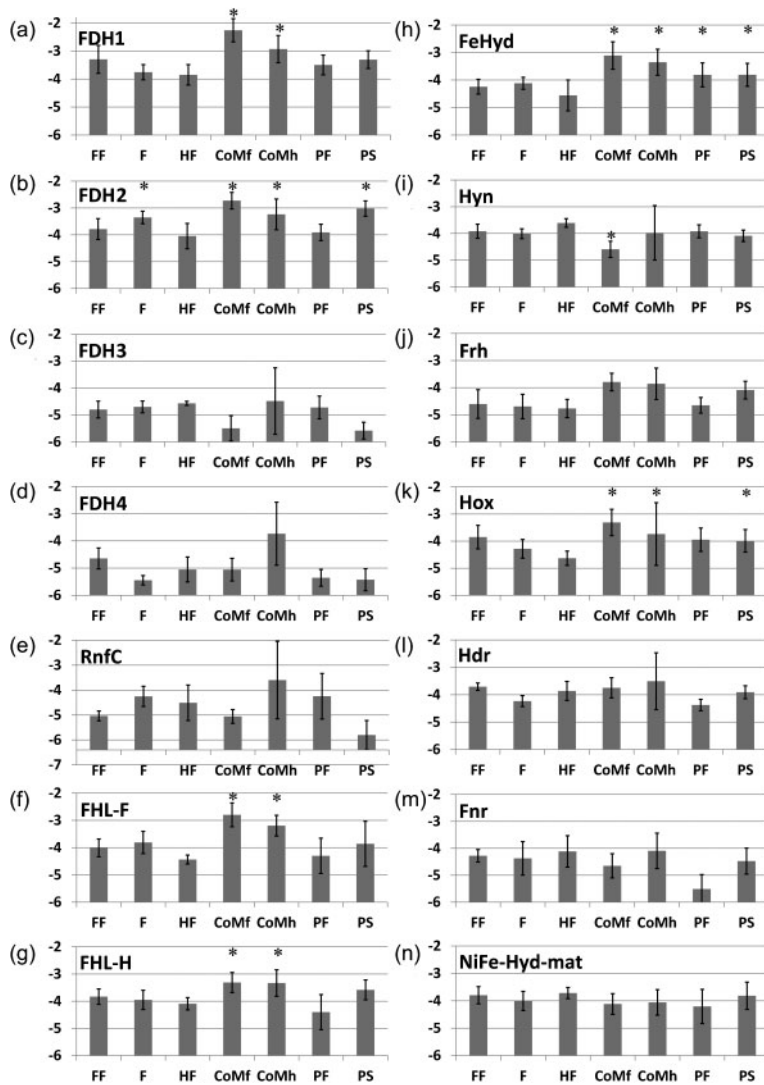


Fig. 2. Transcription of *S. fumaroxidans* genes coding for formate dehydrogenases (a–d), hydrogenases (h–m), RnfC (e), a [NiFe]-hydrogenase maturation protein (n), and formate dehydrogenase (f) and hydrogenase (g) domains of a formate hydrogen lyase. Growth conditions were formate and fumarate (FF), fumarate only (F), hydrogen and fumarate (HF), *S. fumaroxidans* co-culture with *M. formicicum* (CoMf), *S. fumaroxidans* co-culture with *M. hungatei* (CoMh), propionate and fumarate (PF) and propionate and sulfate (PS). The log₁₀ relative transcription levels are shown on the y-axis. *Significant differences; P values are given in the text. Bars show mean ± SD.

pyruvate oxidation, respectively (Chabrière *et al.*, 1999; van Kuijk & Stams, 1996) (Fig. 3). It was proposed that the cytoplasmic FeHyd, FDH1 and Hox confurcate electrons from NADH and reduced ferredoxin to carbon dioxide or protons and generate formate or hydrogen, respectively (Müller *et al.*, 2010; Sieber *et al.*, 2010). Such confurcating enzymes are thus only required when propionate is degraded in pure culture with fumarate or sulfate as electron acceptor and in co-cultures with methanogens. Our results showed increased *feh* and *hox* transcription in propionate-degrading cultures, which is in support of a confurcating function for FeHyd and Hox. Our results suggest that the cytoplasmic formate-producing FDH1 is one of the most important formate dehydrogenases under all conditions and that it is especially induced during syntrophic growth. We hypothesize that FDH1 confurcates electrons from NADH and reduced ferredoxin to produce formate cytoplasmically. The formate could be transported to the methanogen via a formate transporter that is encoded by Sfum_2707 and is located in the operon coding for FDH1 (Müller *et al.* 2010) (Supplementary Fig. S2,

available with the online version of this paper). This would mean that in co-cultures, both hydrogen and formate are transferred, that is generated, in confurcating reactions catalysed by FeHyd, Hox and FDH1 (Fig. 3). Since transcription of *fhl-f* and *fhl-h* is most pronounced during syntrophic growth, hydrogen and formate produced in the cytoplasm will be inter-converted by the formate-hydrogen lyase according to the requirements of the methanogen. Further, genes coding for proteins involved in post-transcriptional maturation of [NiFe]-hydrogenases (such as Hyn and Hox) were found to be important in all growth conditions tested, which corresponds with the observation that genes coding for [NiFe]-hydrogenases were constitutively transcribed.

Transcription of genes involved in electron supply for methanogenesis in *M. hungatei*

At low hydrogen concentration, the first step of the methanogenic pathway is energy dependent and a membrane potential is used to provide enough reduced

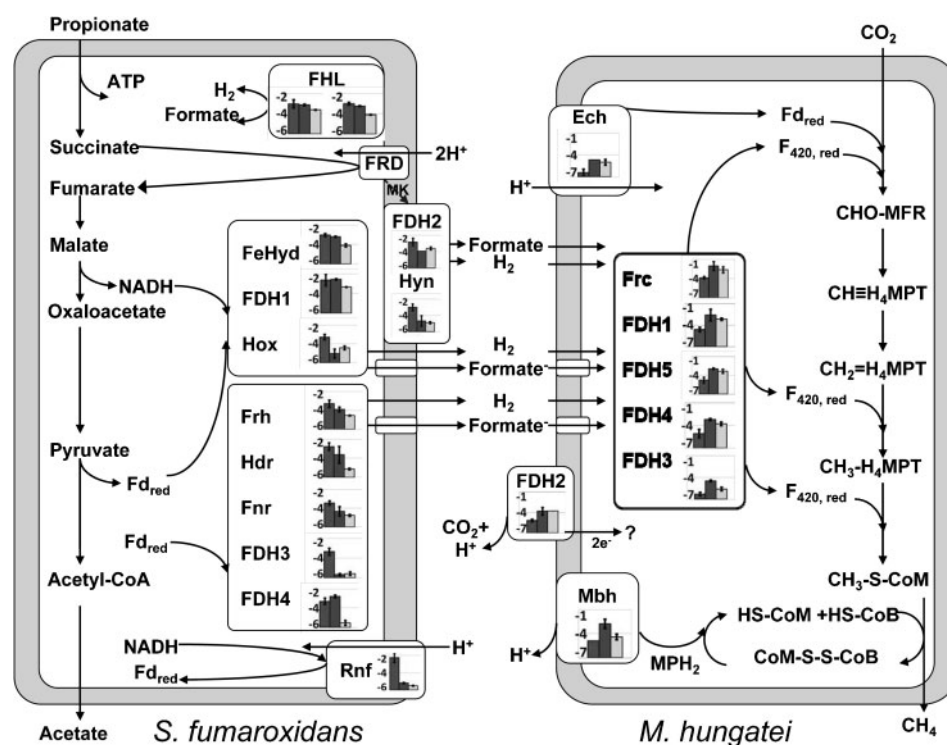


Fig. 3. Formate dehydrogenases and hydrogenases in *S. fumaroxidans* (left) and *M. hungatei* (right) are divided into functional groups. Transcription levels of genes coding for each target enzyme in the three co-cultures of *S. fumaroxidans* and *M. hungatei* (from left to right: CoMh1, CoMh2 and CoMh3, respectively) are shown in the inset graphs, with the log₁₀ relative transcription levels on the y-axis (values are mean ± sd). In CoMh1, in which *S. fumaroxidans* retrieves less energy compared with CoMh2 and -3, the *rnf*-cluster and several ferredoxin-reducing formate dehydrogenases and hydrogenases are induced as a back-up mechanism to reoxidize NADH and ferredoxin efficiently.

ferredoxin to allow reduction of carbon dioxide to formylmethanofuran (Thauer *et al.*, 2008). Membrane-integrated energy-converting hydrogenases (Echs) import protons, cytoplasmically oxidize hydrogen and reduce ferredoxin (Thauer *et al.*, 2008). Thauer *et al.* propose that Echs of methanogens without cytochromes contain at least 16 subunits, whereas the Ech of *Methanosarcina barkeri* – from the order Methanosarcinales and with cytochromes – contains only six subunits. In contrast, our analysis of the genome of *M. hungatei*, which belongs to the Methanomicrobiales, without cytochromes, indicates the presence of a membrane-bound six-subunit Ech (Mhun_1741-46) (Fig. 3, Supplementary Fig. S3). *ech* was transcribed at low levels, possibly to keep interspecies hydrogen concentrations as high as possible.

If formate was the sole electron donor, no hydrogen would be available to oxidize ferredoxin by Ech, and the first step in the methanogenesis would require other enzymes. In *M. hungatei*, this CO₂ reduction is coupled to ferredoxin oxidation (Schwörer & Thauer, 1991). However, its genome indicates the presence of formate dehydrogenases that reduce cofactor F₄₂₀ only. When formate is the

electron donor, the first step of methanogenesis might thus be coupled to cofactor F₄₂₀ oxidation as was reported for *Methanococcus maripaludis* (Hendrickson & Leigh, 2008) (Fig. 3). Electrons from formate possibly flow via a complex that contains FDH, heterodisulfide reductase and MFR-dehydrogenase as was reported for *M. maripaludis* (Costa *et al.*, 2010). Candidates for the oxidation of cofactor F₄₂₀ during MFR reduction, N⁵,N¹⁰-methyl-H₄MPT reduction and N⁵,N¹⁰-methylene-H₄MPT reduction are the cytoplasmic FDH1, -3, -4 and -5 and Frc. *frc* was transcribed in higher levels than *fdh-1*, -3, -4 and -5, which indicates that Frc has the largest contribution. Frc is partly membrane bound (Choquet & Sprott, 1991), which would allow rapid hydrogen consumption. FDH1 might also have a large contribution because it is cotranscribed with a gene coding for a formate transporter (Mhun_1811) that is located in the FDH1 operon (Supplementary Fig. S3 and data not shown). The formate transporter would allow fast import of formate and thus more effective formate oxidation and cofactor F₄₂₀ reduction.

In most Methanomicrobiales, a methylviologen-reducing hydrogenase ADG-HdrABC is involved in hydrogen

oxidation coupled to heterodisulfide reduction, the last step of methanogenesis (Schwörer & Thauer, 1991). However, the genome of *M. hungatei* does not indicate the presence of such an enzyme complex. It also does not contain genes with similarity to a membrane-bound methanophenazine-reducing [NiFe]-hydrogenase, which is involved in the build-up of a membrane potential via hydrogen oxidation in *M. barkeri* (Thauer *et al.*, 2008). Instead, *M. hungatei* contains genes coding for a membrane-bound hydrogenase (Mbh) (Mhun_2579-92) that might be involved in the last step of the methanogenic pathway (Fig. 3).

Interspecies electron transfer in co-cultures of *S. fumaroxidans* with *M. hungatei* or *M. formicicum*

S. fumaroxidans grows in suspended co-cultures with *M. hungatei*, whereas it forms granules in syntrophic growth with *M. formicicum*. It was previously calculated that formate is the preferred interspecies electron carrier in suspended co-cultures and that hydrogen might be preferred when interspecies distances are smaller in granules (Stams & Plugge, 2009). However, no increased transcription of *hyd* genes was observed in *S. fumaroxidans* cells grown with *M. formicicum*. Increased transcription of *fdh* genes was not observed in *S. fumaroxidans* cells grown in syntrophic association with *M. hungatei*. In addition, transcription levels of *hyd* and *fdh* genes in *M. hungatei* were similar in cells grown on hydrogen to those grown on formate. Thus, it could very well be that the same FDHs and HydS allow different electron fluxes and that the presence of certain types of these proteins only reflects the electron flow possibilities.

Hydrogen and formate cycle in pure cultures of *S. fumaroxidans*

When *S. fumaroxidans* uses hydrogen or formate as an electron donor and fumarate as an electron acceptor, Hyn and FDH2 catalyse periplasmic hydrogen and formate oxidation, respectively (Fig. 2b and i). In addition, FHL cytoplasmically inter-converts formate and hydrogen, which are transported to the periplasm via the Foc (Suppmann & Sawers, 1994) and by diffusion, respectively. This explains why Hyn is required during growth on formate and FDH2 is required during growth on hydrogen (Fig. 2b and i). Furthermore, Hyn was downregulated during syntrophic growth and since it is the only periplasmic hydrogenase, it might be the periplasmic component involved in hydrogen cycling. During syntrophic growth, the periplasmically formed hydrogen would be transferred to the methanogen whereas during non-syntrophic growth, an energy conserving hydrogen cycle could exist, as was described for *Desulfovibrio* sp. (Heidelberg *et al.*, 2004; Odom & Peck, 1981).

Metabolic flexibility in co-cultures of *S. fumaroxidans* and *M. hungatei*

Based on the highest formate and hydrogen concentrations maintained by *S. fumaroxidans* and the lowest possible formate and hydrogen concentrations maintained by *M. hungatei*, the formate and hydrogen concentrations in co-cultures vary from 15 to 24 μ M and 2 to 7 Pa, respectively (Dong & Stams, 1995; Schauer *et al.*, 1982; Seitz *et al.*, 1988). Syntrophic partners regulate their metabolism to grow together. The methanogens are favoured if hydrogen and formate concentrations are high, while *Syntrophobacter* requires low hydrogen and formate concentrations. Metabolic flexibility to cope with these fluctuations in hydrogen and formate levels is essential and does occur. The observation that *M. hungatei* cells in CoMh1 contained approximately 10 times more ribosomal activity than *M. hungatei* cells in CoMh2 and -3 (Table 2) reflects this flexibility, though the trigger for it is not yet clear. It also explains why gene transcription values relative to *M. hungatei* 16S rRNA were lower in CoMh1. As a consequence, in CoMh1, *S. fumaroxidans* retrieved less energy for growth and it induced transcription of genes coding for the Rnf-complex, i.e. *fdh* and *hyd* genes. With the assumption that the formate and hydrogen concentrations are high in CoMh1, FDH1 and FeHyd will reduce less carbon dioxide and fewer protons and thus reoxidize less NADH and ferredoxin. This results in the transcription of the genes coding for the third confurcating enzyme, Hox. Moreover, high NADH may lead to the induced transcription of genes coding for the Rnf-complex, which provides the possibility of using the membrane potential for NADH oxidation coupled to ferredoxin reduction. To reoxidize the ferredoxin, the cytoplasmic formate dehydrogenases (FDH3 and -4) and hydrogenases (Frh, Hdr and Frh) are induced in CoMh1 (Fig. 3). In analogy with *S. fumaroxidans* the genomes of other syntrophic fatty-acid-degraders also contain multiple *hyd* and *fdh* genes, and some also have an Rnf-cluster (McInerney *et al.*, 2007; Kato *et al.*, 2009; Müller *et al.*, 2010; Sieber *et al.*, 2010). This suggests that fatty-acid-degraders have numerous possibilities for interspecies electron transfer. To assess the level of metabolic flexibility of each organism in a community, the specific environmental adaptation of syntrophic communities deserves further investigation.

Based on genome analyses and transcriptional profiling, we present here new insight into electron transfer mechanisms and energy conservation in *S. fumaroxidans* and *M. hungatei*. The influence of post-transcriptional regulation in syntrophic communities on the final expression of the proteins still requires further research.

ACKNOWLEDGEMENTS

The research was supported by the Research Councils for Earth and Life Sciences (ALW) and the Chemical Sciences (CW) with financial

aid from the Netherlands Organization for Scientific Research (NWO). We gratefully thank Dr Douwe van der Veen for technical advice.

REFERENCES

- Bagos, P. G., Tsigirigos, K. D., Plessas, S. K., Liakopoulos, T. D. & Hamodrakas, S. J. (2009). Prediction of signal peptides in archaea. *Protein Eng Des Sel* **22**, 27–35.
- Bagramyan, K. & Trchounian, A. (2003). Structural and functional features of formate hydrogen lyase, an enzyme of mixed-acid fermentation from *Escherichia coli*. *Biochemistry (Mosc)* **68**, 1159–1170.
- Burns, M. J., Nixon, G. J., Foy, C. A. & Harris, N. (2005). Standardisation of data from real-time quantitative PCR methods – evaluation of outliers and comparison of calibration curves. *BMC Biotechnol* **5**, 31.
- Chabri re, E., Charon, M. H., Volbeda, A., Pieulle, L., Hatchikian, E. C. & Fontecilla-Camps, J. C. (1999). Crystal structures of the key anaerobic enzyme pyruvate:ferredoxin oxidoreductase, free and in complex with pyruvate. *Nat Struct Biol* **6**, 182–190.
- Choquet, C. G. & Sprott, G. D. (1991). Metal chelate affinity chromatography for the purification of the F_{420} -reducing (Ni,Fe) hydrogenase of *Methanospirillum hungatei*. *J Microbiol Methods* **13**, 161–169.
- Costa, K. C., Wong, P. M., Wang, T., Lie, T. J., Dodsworth, J. A., Swanson, I., Burn, J. A., Hackett, M. & Leigh, J. A. (2010). Protein complexing in a methanogen suggests electron bifurcation and electron delivery from formate to heterodisulfide reductase. *Proc Natl Acad Sci U S A* **107**, 11050–11055.
- de Bok, F. A. M., Luijten, M. L. G. C. & Stams, A. J. M. (2002a). Biochemical evidence for formate transfer in syntrophic propionate-oxidizing cocultures of *Syntrophobacter fumaroxidans* and *Methanospirillum hungatei*. *Appl Environ Microbiol* **68**, 4247–4252.
- de Bok, F. A. M., Roze, E. H. A. & Stams, A. J. M. (2002b). Hydrogenases and formate dehydrogenases of *Syntrophobacter fumaroxidans*. *Antonie van Leeuwenhoek* **81**, 283–291.
- de Bok, F. A. M., Hagedoorn, P. L., Silva, P. J., Hagen, W. R., Schiltz, E., Fritsche, K. & Stams, A. J. M. (2003). Two W-containing formate dehydrogenases (CO_2 -reductases) involved in syntrophic propionate oxidation by *Syntrophobacter fumaroxidans*. *Eur J Biochem* **270**, 2476–2485.
- Dong, X. Z. & Stams, A. J. M. (1995). Evidence for H_2 and formate formation during syntrophic butyrate and propionate degradation. *Anaerobe* **1**, 35–39.
- Harmsen, H. J., van Kwijk, B. L. M., Plugge, C. M., Akkermans, A. D. L., de Vos, W. M. & Stams, A. J. M. (1998). *Syntrophobacter fumaroxidans* sp. nov., a syntrophic propionate-degrading sulfate-reducing bacterium. *Int J Syst Bacteriol* **48**, 1383–1387.
- Heidelberg, J. F., Seshadri, R., Haveman, S. A., Hemme, C. L., Paulsen, I. T., Kolonay, J. F., Eisen, J. A., Ward, N., Methe, B. & other authors (2004). The genome sequence of the anaerobic, sulfate-reducing bacterium *Desulfovibrio vulgaris* Hildenborough. *Nat Biotechnol* **22**, 554–559.
- Hendrickson, E. L. & Leigh, J. A. (2008). Roles of coenzyme F_{420} -reducing hydrogenases and hydrogen- and F_{420} -dependent methyl-ene-tetrahydromethanopterin dehydrogenases in reduction of F_{420} and production of hydrogen during methanogenesis. *J Bacteriol* **190**, 4818–4821.
- Kato, S., Kosaka, T. & Watanabe, K. (2009). Substrate-dependent transcriptomics shift in *Pelotomaculum thermopropionicum* grown in syntrophic co-culture with *Methanothermobacter thermautotrophicus*. *Microb Biotechnol* **2**, 575–584.
- Liu, W. & Saint, D. A. (2002). A new quantitative method of real time reverse transcription polymerase chain reaction assay based on simulation of polymerase chain reaction kinetics. *Anal Biochem* **302**, 52–59.
- McInerney, M. J., Rohlin, L., Mouttaki, H., Kim, U. M., Krupp, R. S., Rios-Hernandez, L., Sieber, J., Struchtemeyer, C. G., Bhattacharyya, A. & other authors (2007). The genome of *Syntrophus aciditrophicus*: life at the thermodynamic limit of microbial growth. *Proc Natl Acad Sci U S A* **104**, 7600–7605.
- McInerney, M. J., Struchtemeyer, C. G., Sieber, J., Mouttaki, H., Stams, A. J. M., Schink, B., Rohlin, L. & Gunsalus, R. P. (2008). Physiology, ecology, phylogeny, and genomics of microorganisms capable of syntrophic metabolism. *Ann N Y Acad Sci* **1125**, 58–72.
- M ller, N., Worm, P., Schink, B., Stams, A. J. M. & Plugge, C. M. (2010). Syntrophic butyrate and propionate oxidation processes: from genomes to reaction mechanisms. *Environ Microbiol Rep* **2**, 489–499.
- Odom, J. M. & Peck, H. D., Jr (1981). Hydrogen cycling as a general mechanism for energy coupling in the sulfate-reducing bacteria, *Desulfovibrio* sp. *FEMS Microbiol Lett* **12**, 47–50.
- Plugge, C. M., Dijkema, C. & Stams, A. J. M. (1993). Acetyl-CoA cleavage pathway in a syntrophic propionate oxidizing bacterium growing on fumarate in the absence of methanogens. *FEMS Microbiol Lett* **110**, 71–76.
- Schauer, N. L., Brown, D. P. & Ferry, J. G. (1982). Kinetics of formate metabolism in *Methanobacterium formicicum* and *Methanospirillum hungatei*. *Appl Environ Microbiol* **44**, 549–554.
- Schink, B. & Stams, A. J. M. (2006). Syntrophism among prokaryotes. *Prokaryotes* **2**, 309–335.
- Sch t, G. J. & Adams, M. W. W. (2009). The iron-hydrogenase of *Thermotoga maritima* utilizes ferredoxin and NADH synergistically: a new perspective on anaerobic hydrogen production. *J Bacteriol* **191**, 4451–4457.
- Schw rer, B. & Thauer, R. K. (1991). Activities of formylmethanofuran dehydrogenase, methylene-tetrahydromethanopterin dehydrogenase, methylene-tetrahydromethanopterin reductase, and heterodisulfide reductase in methanogenic bacteria. *Arch Microbiol* **155**, 459–465.
- Seitz, H. J., Schink, B. & Conrad, R. (1988). Thermodynamics of hydrogen metabolism in methanogenic cocultures degrading ethanol or lactate. *FEMS Microbiol Lett* **55**, 119–124.
- Sieber, J. R., Sims, D. R., Han, C., Kim, E., Lykidis, A., Lapidus, A. L., McDonald, E., Rohlin, L., Culley, D. E. & other authors (2010). The genome of *Syntrophomonas wolfei*: new insights into syntrophic metabolism and biohydrogen production. *Environ Microbiol* **12**, 2289–2301.
- Stams, A. J. M. & Plugge, C. M. (2009). Electron transfer in syntrophic communities of anaerobic bacteria and archaea. *Nat Rev Microbiol* **7**, 568–577.
- Stams, A. J. M., Van Dijk, J. B., Dijkema, C. & Plugge, C. M. (1993). Growth of syntrophic propionate-oxidizing bacteria with fumarate in the absence of methanogenic bacteria. *Appl Environ Microbiol* **59**, 1114–1119.
- Suppmann, B. & Sawers, G. (1994). Isolation and characterization of hypophosphite-resistant mutants of *Escherichia coli*: identification of

the FocA protein, encoded by the *pfl* operon, as a putative formate transporter. *Mol Microbiol* **11**, 965–982.

Thauer, R. K., Kaster, A. K., Seedorf, H., Buckel, W. & Hedderich, R. (2008). Methanogenic archaea: ecologically relevant differences in energy conservation. *Nat Rev Microbiol* **6**, 579–591.

van Doesburg, W., van Eekert, M. H. A., Middeldorp, P. J. M., Balk, M., Schraa, G. & Stams, A. J. M. (2005). Reductive dechlorination of β -hexachlorocyclohexane (β -HCH) by a *Dehalobacter* species in

coculture with a *Sedimentibacter* sp. *FEMS Microbiol Ecol* **54**, 87–95.

van Kuijk, B. L. M. & Stams, A. J. M. (1996). Purification and characterization of malate dehydrogenase from the syntrophic propionate-oxidizing bacterium strain MPOB. *FEMS Microbiol Lett* **144**, 141–144.

Edited by: H. L. Drake